Applied Engineering Letters Vol.3, No.1, 6-12 (2018) e-ISSN: 2466-4847

FAILURE MODE AND STRENGTH ANALYSES OF RESISTANCE SPOT WELD JOINTS OF ALUMINIUM AND AUSTENITIC STAINLESS STEEL SHEET

UDC: 621.79
Original scientific paper https://doi.org/10.18485/aeletters.2018.3.1.2

Aleksija Đurić[1], Biljana Marković[1]

[1]University of East Sarajevo, Faculty of Mechanical Engineering, Bosnia and Herzegovina

Abstract:
Resistance spot welding (RSW) is considered as the dominant process for joining similar and dissimilar sheet metals in automotive industry. In this paper will be present the strength analyses of spot weld joint and analyse the transition between interfacial and pull-out failure modes for resistance spot weld joints of aluminium and austenitic stainless steel sheet, during the tensile–shear test, by usage analytical and experimental approach. For experimental testing, the specimen of 1 mm and 2 mm thickness were used, welded with different welding parameters.

ARTICLE HISTORY
Received 11.01.2018
Accepted 26.02.2018
Available 15.03.2018

KEYWORDS
resistance spot welding, failure mode, tensile-shear test

1. INTRODUCTION

Lightweight design (LW) is resulting from the need for sustainable design and product development [1]. Material, design and manufacturing technologies remain key technologies in vehicle development [2] and also in other products development. The essence of success at global world market is integration, so the multi-material design has been developed as a modern concept of LW design, aimed at integrating different types of materials into one structure. For example, vehicle body weight can be reduced using multiple materials without cost increase [3]. Various lightweight automotive bodies have been developed using high strength steels, aluminium alloys, and composite materials. One prerequisite for multi-material structures for car bodies is the availability of material-capable and cost-efficient joining technologies [4].

Aluminium, aluminium alloys, and steel are often used in multi-material structures, so there are various studies [4,5] that analyse how these materials are bonded. Very often in these studies can be saw the resistance spot welding (RSW) [6-8] as one solution. Despite the emergence of new technologies, RSW is still a dominant process for joining similar and dissimilar sheet metals in automotive industry.

Joint failure, e.g. resistance spot weld (RSW) joint failure, was identified as one of the key failure types when a vehicle crash occurs [9]. Failure mode of resistance spot welds is indicator of weld quality. Two major types of spot weld failure are pull-out and interfacial fracture [9,10]. The aim of this paper is strength analyse of spot weld joint and analyse the transition between interfacial and pull-out failure modes for resistance spot weld joints of aluminium 99,5 (1050A) and austenitic stainless steel X2CrNi18-9 sheet during the tensile–shear test, using analytical and experimental approach.

Austenitic stainless steels, and therefore the steel X2CrNi18-9 is often used as construction material in the chemical- and food-processing industry [11] and also, this steel is applied in the automotive industry [12]. In order to develop lightweight structures, stainless steel is tended to replace, primarily because of their weight. However, steel structures cannot be completely replaced, it is possible to replace parts of constructions with lightweight materials, such as aluminium. In this case, it is necessary to join stainless steels and aluminium [13]. The chemical composition and basic mechanical properties of steel X2CrNi18-9 and aluminium 99.5 (1050A), that

CONTACT: Aleksija Đurić, aleksijadjuric@gmail.com

were used for research present in this paper, are given in Table 1.

Table 1. Chemical composition and basic mechanical properties of steel X2CrNi18-9 and aluminum 99.5 (1050A)

Material	Steel X2CrNi18-9		Al99,5	
Chemical composition [%]	C	0,03	Al	99,5
	Si	0,75	Si	0,25
	Mn	2,0	Fe	0,4
	Ni	8,0	Cu	0,05
	Cr	17,5	Mn	0,05
	N	0,1	Mg	0,05
	S	0,015	Zn	0,07
	P	0,045	Ti	0,05
Mech. properties	R_m [N/mm^2]	540	R_m [N/mm^2]	230
	$R_{p0,2}$ [N/mm^2]	100-135	$R_{p0,2}$ [N/mm^2]	75
	HB	92	HB	35

2. TEORETYCL STRESS ANALYSES AND FAILURE MODE TRANSITION

Basically, spot welds can fail in three distinct different modes, shown on Fig.1, described as follows [9]:

- Interfacial failure (IF) in which, fracture propagates through the fusion zone (FZ)
- Pull-out failure (PF) in which, failure occurs via the withdrawal of weld nugget from one sheet. In this mode, fracture may initiate in base metal (BM), heat affected zone (HAZ) or HAZ/FZ depending on the base metal and the loading condition.
- Partial interfacial mode (PIF) in which, fracture first propagates in fusion zone (FZ) and then is redirected through thickness.

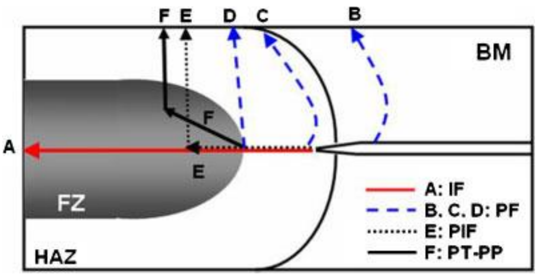

Fig.1. Schematic of various failure modes during mechanical testing [14]

The failure of resistance spot welds during the tensile–shear test can be described as a competition between the shear plastic deformation of the fusion zone (i.e. IF mode) and the necking in the base metal (i. e. PF mode) [9]. At the nugget circumference, shown on Fig.2, stresses are shear tensile at position A and shear compression at position B [10].

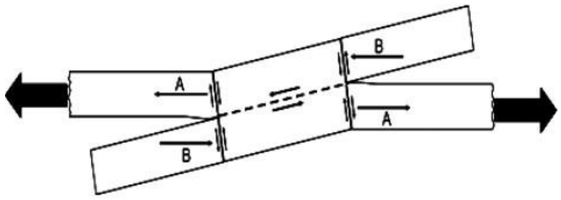

Fig.2. Distribution at nugget centerline and circumference during shear tensile test [16]

According to [9] the failure load at the interfacial failure mode (IF mode) can be expressed using Eq. 1:

$$F_{IF} = \frac{\pi}{4} \cdot d^2 \cdot \tau_{FZ} \quad (1)$$

where d is the diameter of the weld nugget and the τ_{FZ} is shear strength of the fusion zone.

For PM mode, failure is initiated when the maximum experienced radial tensile stress at nugget circumference reaches the ultimate tensile strength of the failure location. Therefore, failure load in the PF mode can be expressed using Eq. 2 [9]:

$$F_{PF} = \pi \cdot t \cdot d \cdot \sigma_{PFL} \quad (2)$$

where t is the thickness of the base metal sheet and σ_{PFL} is the ultimate tensile strength of the PF location.

For Sawhill and Baker, equation 2 can be written as Eq. 3 [10]:

$$F_{PF} = c \cdot t \cdot d \cdot \sigma_{BM} \quad (3)$$

Where σ_{BM} is the ultimate tensile strength of base material and c is a constant between 2,5 and 3,1.

According to previous equations, the comparative stress of spot weld joint can be calculated using Eq. 4:

$$\sigma_s = \max\left\langle \frac{4F}{i \cdot \pi \cdot d^2} \cdot \frac{1}{\alpha_1}, \frac{F}{i \cdot \pi \cdot t \cdot d} \cdot \frac{1}{\alpha_2} \right\rangle \quad (4)$$

where F is applied load, i number of welds and α coefficient of weld joint. Coefficient α_1 is 0,65 and α_2 is 0,5 [15].

Comparative stress is approach to calculate stresses in spot weld joint. Generally, the stress in welds has normal and tangential components. The method of comparative stresses is based on the fact that the shear strength of weld metal is lower than the tensile strength [15].

3. EXPERIMENTAL PROCEDURE

Specimens for this study are prepared in accordance with EN ISO 14273: 2001, the dimensions of specimens are shown on Fig.3.

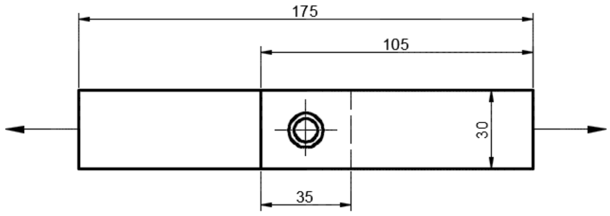

Fig.3. Dimensions of specimen

The process of spot welding was done on the machine shown in Fig.4, manufactured by DALEX WERK, located in the TMD dommers factory in Gradačac, BiH. Welding parameters for all specimens are given in Table 2. For the welding of all specimen, class 2 electrodes (Cu + Zr + Cr) were used. The head of the upper electrode is 5 mm and the lower electrode type is beck-up. Also, the electrode force for all specimens was 2 kN.

Fig.4. Spot weld machine and specimen after spot welding

For further analysis, it is very important to know which material is in contact with the upper electrode. Steel and aluminum are not the same conductors of electricity, so different parameters are required in welding if the same quality of welding is desired. It is visually possible to perceive the difference in the appearance of the weld, depending on that which material is in a contact with the upper electrode, as shown in Fig.5.

The tensile -shear test of all specimens welded by RSW with welding parameters shown in Table 2., was carried out according to the recommendations of the aforementioned standard EN ISO 14273: 2001, on the test machine AGS-X 20 kN, manufactured by SCHIMDZU (Fig.6).

Table 2. Welding parameters for all specimens

Marks	Mat. 1	Mat. 2	Thic. 1 t [mm]	Thic. 2 t [mm]	Weld current [kA]	Weld time [1/100 sec]	Number and position of weld
E24	Al 99,5	X2CrNi18-9	1	1	6	32	*
E26			1	1	6	32	*
E27			1	1	6	32	*
E28**			1	1	6	32	* *
E29**			1	1	6	32	* *
E30			1	1	6	32	* *
E40			1	1	6	32	* *
E32*			2	1	7	32	*
E33*			2	1	7	32	*
E34			2	1	7	32	*
E35			2	1	7	32	*
E49			2	1	7	72	* *
E50			2	1	7	72	* *
E51			2	1	7	72	* *

* The steel was in direct contact with the upper electrode
** For one spot steel was in contact with the upper electrode and for other one spot aluminum was in contact with the upper electrode

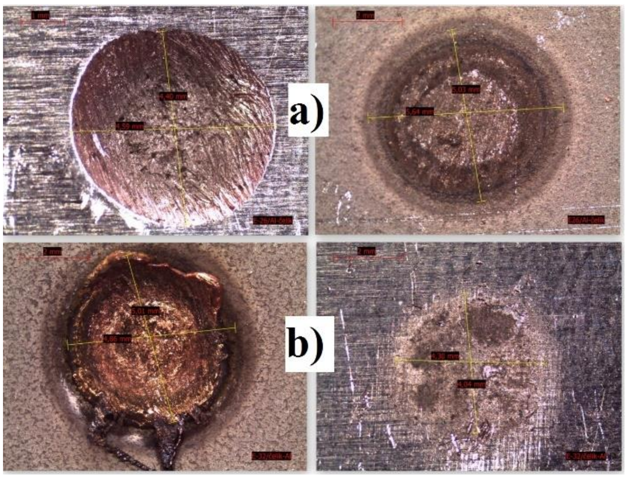

Fig.5. a) Spot weld when aluminum is in a contact with upper electrode; b) Spot weld when steel is in a contact with upper electrode

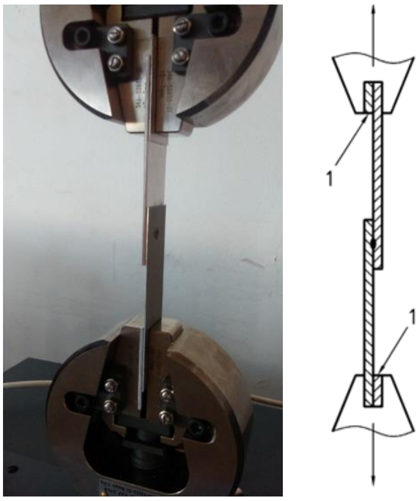

Fig.6. Specimen prepared for testing set in jaws of test machine (1- shim plates)

4. RESULTS AND DISCUSSION

In this section it will be shown illustration of two major types of spot weld failure: pull-out (PF) and interfacial fracture (IF) and tensile-shear strength for previously shown specimens.

Pull-out failure (PF) is illustrated in Fig.6a for all three specimens marked as E24, E26 and E27. These are specimens with one spot and sheet thickness of both materials (aluminum and steel) of 1 mm. In standard EN ISO 14273:2001 pull-out failure shown on Fig.7a is called spot weld with partial pull-out failure.

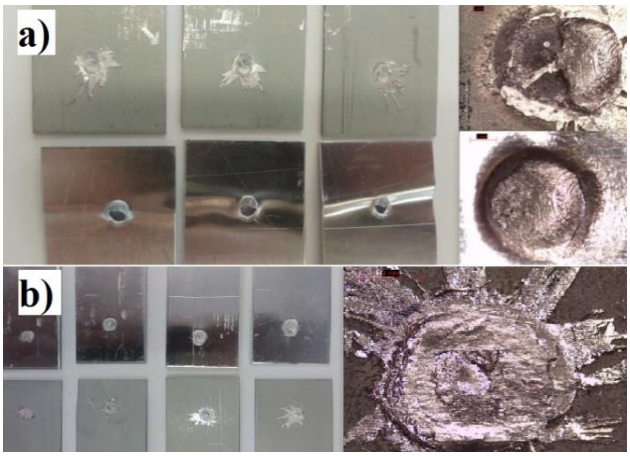

Fig.7. Illustration of failures: a) pull-out failure (PF); b) interfacial failure (IF)

A specimen with one spot with aluminum thickness of 2 mm, and steel 1 mm marked E32-E35 after the testing are shown on Fig.6b, where interfacial failure (IF) can be seen. The force/displacement diagram for the E24 specimen for static tensile-shear test is shown in Fig.8.

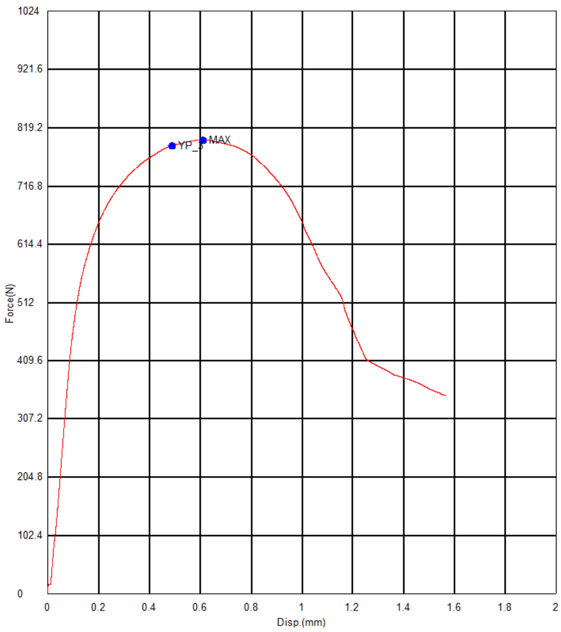

Fig.8. Force/displacement diagram for the E24 specimen

Specimens marked with E32 and E33 were welded so that the steel was in contact with the upper electrode, and the specimens E34 and E35 were welded so that the aluminum was in contact with the upper electrode. In terms of failure mode, this is not important. Fig.9a shows the force/displacement diagram for E32 specimen (steel in contact with the upper electrode) and Fig. 9b shows same diagram for E35 specimen (aluminum in contact with the upper electrode).

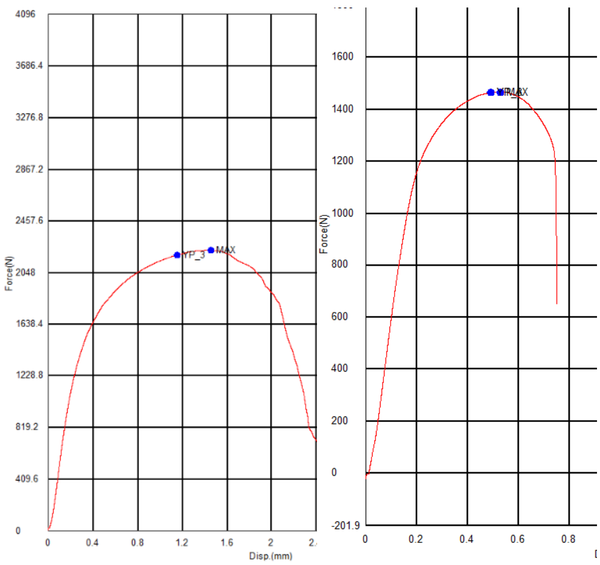

a) b)

Fig.9. Force/displacement diagram for the a) E32 specimen; b) E35 specimen

The fact that the specimens E32 and E33 were welded so that steel is in contact with the upper electrode was shown as a favorable case in terms of a tensile shear straight, what can be concluded when comparing Fig.9a and 9b.

One of very important parameter for spot weld obtained from force/displacement curves is energy absorption [16,17]. The amount of energy absorption can be digitally calculated by measuring the area under the force/displacement curve up to failure using the Eq. 5 [16]:

$$Q = \sum_{n=1}^{N} F(n) \cdot [x(n) - x(n-1)] \tag{5}$$

where F is force, x the displacement, n the sampled data and N the peak failure load.

Load carrying capacity and energy absorption capability for those welds fail under interfacial mode, are much less than those which fail under pull-out mode. To ensure reliability of spot welds during vehicle lifetime, process parameters should be adjusted so that pull-out failure mode is guaranteed [10].

When the spot weld joint is with two spots, for the same specimen thickness, the fail is dominant in the PF mode, regardless of whether the spots are arranged vertically or horizontally (Fig.10a). For the same spot weld joint, but with different thickness of aluminum (2 mm) and steel (1 mm), the fail is dominant in the IF mode (Fig.10b).

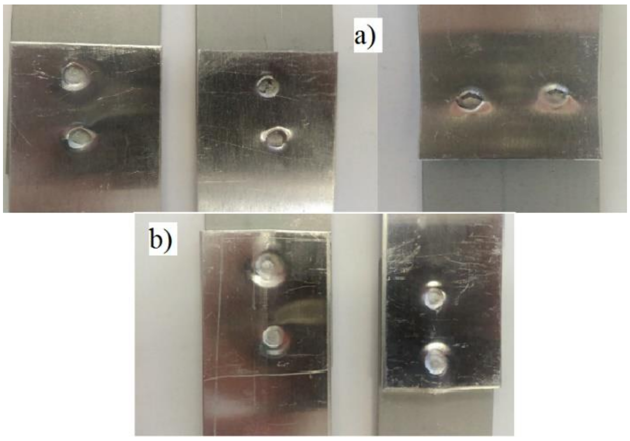

Fig.10. Illustration of a) pull-out failure (PF); b) interfacial failure (IF) for spot weld with two spots

The tensile-shear strength of the specimens with the vertical spots marked E28 and E29 is somewhat higher than the specimens with horizontal spots E30 and E40, although the same welding parameters. One of the reasons is the fact that for a vertical weld joint one spot is welded when aluminum being in contact with the upper electrode and other one when steel being in contact with the upper electrode, differing from the horizontal layout, where both spots are welded when aluminum being in contact with the upper electrode.

The values of tensile-shear strength and comparative stress for all specimens are shown in Table 3.

Tensile-shear strength of specimen marked E49 i E50 is higher than tensile-shear strength of E28 i E29 specimens, especially because of different thickness, weld current and weld time. This four specimens have same layout of spots. The force/displacement diagram for the E29 specimen is shown in Fig.11a and for the E50 specimen is shown in Fig.11b.

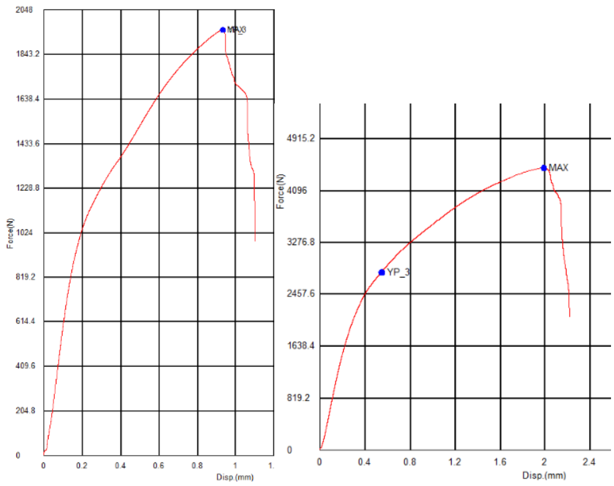

Fig.11. Force/displacement diagram for the a) E29 specimen; b) E50 specimen

The influence of the weld time on the tensile-shear strength was shown in [18] and the analysis in [19] shows the percentage contribution of individual parameters on the weld strength. The percentage contribution of the welding current is 49.81%, the thickness of 37.94% and the cycle time of 2.61%.

The analytically obtained stress values based on equation 4 shown in Table 3 confirm the previous experimental test, in terms of failure mode. For example, specimens E24 to E30 and E40 have higher stress analytically obtained for PF mode, than stress analytically obtained for IF mode. Also, previous Figures (Fig.7a and Fig.10a) confirm that these specimens fail in PF mode in experimentally test.

Table 3. The values of tensile-shear strength and comparative stress

Mar.	F_{max} [N]	i	$\frac{4F}{i\cdot\pi\cdot d^2}\cdot\frac{1}{\alpha_1}$ [N/mm^2]	$\frac{F}{i\cdot\pi\cdot t\cdot d}\cdot\frac{1}{\alpha_2}$ [N/mm^2]	σ_s [N/mm^2]
E24	797,494	1	62,52	101,59	101,59
E26	771,043	1	60,44	98,22	98,22
E27	811,536	1	63,62	103,38	103,38
E28	2203,63	2	86,37	140,36	140,36
E29	1996,20	2	78,24	127,15	127,15
E30	1347,91	2	52,83	85,85	85,85
E40	1665,5	2	65,28	106,08	106,08
E32	2224,33	1	174,37	141,68	174,37
E33	2073,79	1	162,57	132,09	162,57
E34	1645,35	1	128,98	104,80	128,98
E35	1472	1	115,39	93,76	115,38
E49	4380,55	2	171,70	139,51	171,70
E50	4453,22	2	174,55	141,82	174,55
E51	2810,55	2	110,16	89,51	110,16

5. CONCLUSION

In this paper was analyzed the tensile-shear strength and failure mode of the spot weld joint of X2CrNi18-9 steel and aluminum 99.5. The theoretical analysis was showed, that spot welds for tensile-shear load general can fail in two distinct different modes: IF (Interfacing) in which, fracture propagates through the fusion zone (FZ) and pull-out failure (PF). The analytical comparative stress of the spot weld joint is determined by selecting the maximal value between the stresses received by the IF and the PF mode.

The experimental testing of the spot weld joint of the aforementioned two materials for different welding parameters and the thickness of the material was done, as a confirmation of the theoretical analysis. After the experiment, it is easy to recognize which mode belongs to the fail of the specimen and it was found that comparative stress is analytical obtained from the same failure mode. The thickness of the material is one of the parameters that largely indicate in which failure mode will fail spot weld joint.

Many previous studies, referenced here, together with this one shown that, in terms of the tensile-shear, the strength material thickness and the welding current are very important. Also, the tensile-shear strength depends on which material is in contact with upper electrode, when dissimilar material welding, which has been shown here.

REFERENCES

[1] A. Đurić, B. Marković, N. Vučetić, S. Pelkić, Calculation of factors LBKz and its significance for the development of light weight construction. In The 3rd International Conference - "Mechanical Engineering in XXI Century", September 2015, Niš, Serbia, pp.17-18.

[2] M. Goede, M. Stehlin, L. Rafflenbeul, G. Kopp, E. Beeh, Super Light Car-lightweight construction thanks to a multi-material design and function integration. *European Transport Research Review*, 1 (1), 2009: 5-10. https://doi.org/10.1007/s12544-008-0001-2

[3] X. Cui, H. Zhang, S. Wang, L. Zhang, J. Ko, Design of lightweight multi-material automotive bodies using new material performance indices of thin-walled beams for the material selection with crashworthiness consideration. *Materials & Design*, 32 (2), 2011: 815-821. http://dx.doi.org/10.1016/j.matdes.2010.07.018

[4] G. Meschut, V. Janzen, T. Olfermann, Innovative and highly productive joining technologies for multi-material lightweight car body structures. *Journal of Materials Engineering and Performance*, 23 (5), 2014: 1515-1523. https://doi.org/10.1007/s11665-014-0962-3

[5] T. Sakiyama, G. Murayama, Y. Naito, K. Saita, Y. Miyazaki H. Oikawa, T. Nose, Dissimilar metal joining technologies for steel sheet and aluminum alloy sheet in auto body. *Nippon Steel Technical Report*, (-) 103, 2013: 91-98.

[6] B. X. Sun, E. V. Stephens, M. A. Khaleel, H. Shao, M. Kimchi, Resistance spot welding of aluminum alloy to steel with transition material-from process to performance-Part I: experimental study. *Welding Journal*, 83 (-), 2004: 188-195.

[7] R. Qiu, C. Iwamoto, S. Satonaka, Interfacial microstructure and strength of steel/aluminum alloy joints welded by resistance spot welding with cover plate. Journal of Materials processing technology, 209 (8), 2009: 4186-4193. https://doi.org/10.1016/j.jmatprotec.2008.11.003

[8] W. H. Zhang, X. M. Qiu, D. Q. Sun, L. J. Han, Effects of resistance spot welding parameters on microstructures and mechanical properties of dissimilar material joints of galvanised high strength steel and aluminium alloy. *Science and Technology of Welding and Joining*, 16 (2), 2011: 153-161. https://doi.org/10.1179/1362171810Y.0000000009

[9] M. Pouranvari, S. P. H. Marashi. Failure mode transition in AHSS resistance spot welds. Part I. Controlling factors. *Materials Science and Engineering: A*, 528 (29-30), 2011: 8337-8343. https://doi.org/10.1016/j.msea.2011.08.017

[10] M. Pouranvari, H. R. Asgari, S. M. Mosavizadch, P. H. Marashi, M. Goodarzi, Effect of weld nugget size on overload failure mode of resistance spot welds. *Science and Technology of Welding and Joining*, 12 (3), 2007: 217-225. https://doi.org/10.1179/174329307X164409

[11] D. Müller, G. K. Wolf, B. Stahl, L. Amaral, M. Behar, J. B. M. da Cunha, Phase transformation and corrosion behavior of stainless steel bombarded by pulsed energetic ion beams. *Surface and Coatings Technology*, 158-159 (-), 2002: 604-608. https://doi.org/10.1016/S0257-8972(02)00318-3

[12] P.-J. Cunat, Stainless steel in structural automotive applications. No.2002-01-2067. SAE Technical Paper, 2002.

[13] S. Fukumoto, H. Tsubakino, K. Okita, M. Aritoshi, T. Tomita, Friction welding process of 5052 aluminium alloy to 304 stainless steel. *Materials Science and Technology*, 15 (9), 1999: 1080-1086. https://doi.org/10.1179/026708399101506805

[14] M. Pouranvari, S. P. H. Marashi, S. M, Mousavizadeh, Failure mode transition and mechanical properties of similar and dissimilar resistance spot welds of DP600 and low carbon steels. *Science and Technology of Welding and Joining*, 15 (7), 2010: 625-631. https://doi.org/10.1179/136217110X12813393169534

[15] https://www.engineersedge.com/weld/spot weld_joint_single_shear.htm. (Accept 26.07.2017.)

[16] M. I. Khan, M. L. Kuntz, and Y. Zhou, Effects of weld microstructure on static and impact performance of resistance spot welded joints in advanced high strength steels. *Science and Technology of Welding and Joining*, 13 (3) 2008: 294-304. https://doi.org/10.1179/174329308X271733

[17] L. Han, M. Thornton, M. Shergold, A comparison of the mechanical behaviour of self-piercing riveted and resistance spot welded aluminium sheets for the automotive industry. *Materials & Design*, 31 (3), 2010: 1457-1467. http://dx.doi.org/10.1016/j.matdes.2009.08.031

[18] S. Aslanlar, A. Ogur, U. Ozsarac, E. Ilhan, Welding time effect on mechanical properties of automotive sheets in electrical resistance spot welding. *Materials & Design*, 29 (7), 2008: 1427-1431. https://doi.org/10.1016/j.matdes.2007.09.004

[19] D.Shah, D.P. Patel, Prediction of weld strength of resistance spot welding using artificial neural network. *Journal of Engineering Research and Application*, 3 (5), 2013: 1486-1491.

The shorter version of this research was presented at the "8nd International Scientific Conference IRMES 2017", 7 - 9 September 2017, Trebinje, Bosnia and Hercegovina.